

Detecting Excitations of Pipes, Ropes, and Bars by Piezo Sensors and Collecting Information in Remote

Matteo Cirillo ^{1,*}, Enzo Reali ² and Giuseppe Soda ³

¹ Dipartimento di Fisica and MINAS Lab, Università di Roma “Tor Vergata”, 00133 Roma, Italy

² Dipartimento di Fisica, Università di Roma “Tor Vergata”, 00133 Roma, Italy; reali@roma2.infn.it

³ Pipe Monitoring Corporation, PIMOC, via Cola di Rienzo 212, 00192 Roma, Italy; pinogsoda@gmail.com

* Correspondence: cirillo@roma2.infn.it; Tel.: +390672594518

Abstract: An investigation of a non invasive method to detect defects and localize excitations in metallic structures is presented. It is shown how signals generated by very sensitive piezo sensors assemblies, secured to the metallic elements, can allow space localization of excitations and defects in the analyzed structures. The origin of the piezo excitations are acoustic modes generated by light percussive excitations whose strength is of the order of tenths of newton and provide piezo signal amplitudes of few hundred millivolts. Tests of the detection scheme of the excitations are performed on steel ropes, iron pipes and bars having lengths in the range (1–6) m with the sensor output signal shaped in a form of a clean pulse. It is shown that the signals generated by the piezo assemblies, adequately shaped, can feed the input of an RF transmitter which in turn transfers information to a remote receiver whose readout allows analyzing in remote the information collected on the metallic elements. Considered the voltage amplitude of the signals (of the order of 300 mV) generated by the piezo sensors as result of very light percussive excitations, the low power required for transmitting data, and the low cost of the sensing and transmitting assembly, it is conceivable that our devices could detect excitations generated even tens of kilometers away and allow setting up array of sensors for controlling in real time the status of pipe networks.

Keywords: piezoelectric sensors; pipes monitoring; signal handling and transmission, pulse transmission, acoustic excitations

1. Introduction

Piezoelectric sensors and devices cover wide ranges of applications in fundamental science, engineering and technology [1, 2, 3] and represent a unique tool when the issue is to detect very small displacements and excitations of solid bodies [4]. Nowadays at least three relevant fields for possible applications of piezo devices exist and our efforts are targeted on proposing possible solutions. From the type of application the reason why we will herein concentrate experiments on specific shapes/geometries of the metallic elements will be clear.

The first issue motivating our interest is monitoring the security of oil and gas pipelines: this is a problem of paramount relevance for avoiding frauds, and related environmental disasters, along conducts taking oil, or gas, from sources to refineries or from refineries to distributors [5–11]. The frauds are committed by producing holes in the pipelines from which the product is extracted. This criminal activity produces economic and environmental damages quantifiable in the order of several hundred million dollars per year. Setting up a reliable protocol for detecting, in real time, harmful operations on the pipelines would constitute a relevant progress for the safety of oil/gas distribution. Naturally, the system to be set up for the detection must consider the fact that pipelines length can be thousands of kilometers and transmission of the signals of the sensors to adequate receivers must go through ether. At this time a system monitoring from remote the status of pipelines networks and providing information in real time on the location/origin of the problems does not exist.

Citation: To be added by editorial staff during production.

Academic Editor: Firstname Last-name

Received: date

Revised: date

Accepted: date

Published: date



Copyright: © 2024 by the authors. Submitted for possible open access publication under the terms and conditions of the Creative Commons Attribution (CC BY) license (<https://creativecommons.org/licenses/by/4.0/>).

Another relevant issue concerning the localization of defects in metals and cables is the control of the status of rail tracks [12-17] and steel ropes of cable cars [18-23]. In both these cases a sensitive and non-invasive system for localizing, well ahead of problems, the quality and the status of ropes and rail tracks would be extremely helpful and prevent problems due to cracks and defects. A terrible accident which happened in Italy on the Stresa Mottarone cable car in May 2021 has attracted much attention on the research for defects localization on the ropes. The ropes that we use are those also provided for cable car construction. The high velocities achieved by trains, however, also require paramount attention on the quality, performances, and status of conservation of the rail tracks.

Finally, degradation of iron and steel embedded in concrete is a problem also gathering much attention from the structural engineering side [24-28]. This problem has become particularly important in Italy after the Morandi bridge disaster in Genova in August 2018. Authors of the present publication have active collaborations with highways construction companies (ANAS, TOTO Construction) in order to find possible solutions of the problem, namely checking the status of the steel embedded in concrete structures [29].

For the physical cases, and necessities, described above the primary requirements in the search of detection systems are adequate sensitivity, reliability, the possibility of operating over long distances the sensor devices and, naturally, the possibility to collect information in remote. In the present paper it is described how a piezoelectric assembly, requiring very limited power for its operation, could allow detecting defects of bars, ropes, and pipelines and also to localize the presence of external excitations along these structures. The basic principle for all cases is the detection of acoustic excitations. The signals generated by the piezo units caused by the excitations are transformed in rectangular impulses and time delays associated with them allow determining the presence of defects and excitations. It is also shown how the impulses generated by our measurement protocol are transmitted through the ether and received in remote to handle the information. Evidence will be provided that our sensor devices and detection system have all the ingredients necessary for application to cases of noticeable interest.

The remainder of the paper is structured as follows. In the next section the basic hardware and the detection principle of the sensor assembly is described and it is shown that it can detect very weak signals when secured to steel pipes; in sect. 3 it is demonstrated how the signals of the sensors can be treated to generate clean pulses allowing straight detection of time delays and transmission of information at large distances. The pulses originated by the piezos as described in sect. 3 are then employed to characterize pipes, bars, and ropes in sect. 4. In sect.5 evidence of excitations and defects localization by our measuring protocol is provided in steel ropes and bars. In sect. 6 we draw the conclusions of our work.

2. The Sensor Assembly

In Fig. 1a the mounting assembly of our piezo sensor is shown. The piezo element is fixed on a Printed Circuit Board (PCB) by holding it in mechanical contact with two pieces of metal (the fixers): the piezo and its fixers are shown by arrows in the figure. A tiny amount of silver paste (Agar Quick drying g3020) is used for enhancing the contact between piezo and fixers. The piezo elements we used were part of a stock purchased from the company Riccardo Beyerle s.p.a. (Italy). The piezos material is described in ref. 30 and specifically of the type $\text{Pb}(\text{Zr}_{0.52}\text{Ti}_{0.48})\text{O}_3$. The role of the fixers is, beside firmly positioning the piezo on the board, to transmit the mechanical stresses to the piezo: the two metal fixers contacting the piezo are secured by three screws (S1, S2, and S3 on the photo) to the PCB and these are tightened up by a nut on the back of the board as shown in Fig. 1b. The photo of Fig. 1a also shows part of the LEMO cable collecting the signal from the piezo element. Fig. 3c shows a cross section of the assembly on a 0.23 m-diameter pipe.

The assembly of Fig. 1a,b was covered by a plastic case and firmly tight by robust tape on an iron flat metal plate ($l=14$ cm, $w=4$ cm, $t=0.4$ cm) as shown in Fig. 1c. The three

screws shown in Fig. 1b as S1, S2, and S3 contact the metal plate, which we call “transmission plate”; this plate, in turn, is secured to the metallic elements whose excitations we intend to trace by placing two strong parallelepiped-shaped magnets ($l=3\text{cm}$, $w=1\text{cm}$, $t=0.5\text{cm}$) between the transmission plate and the metallic elements. The used magnet generates a field $B=0.45\text{ T}$.

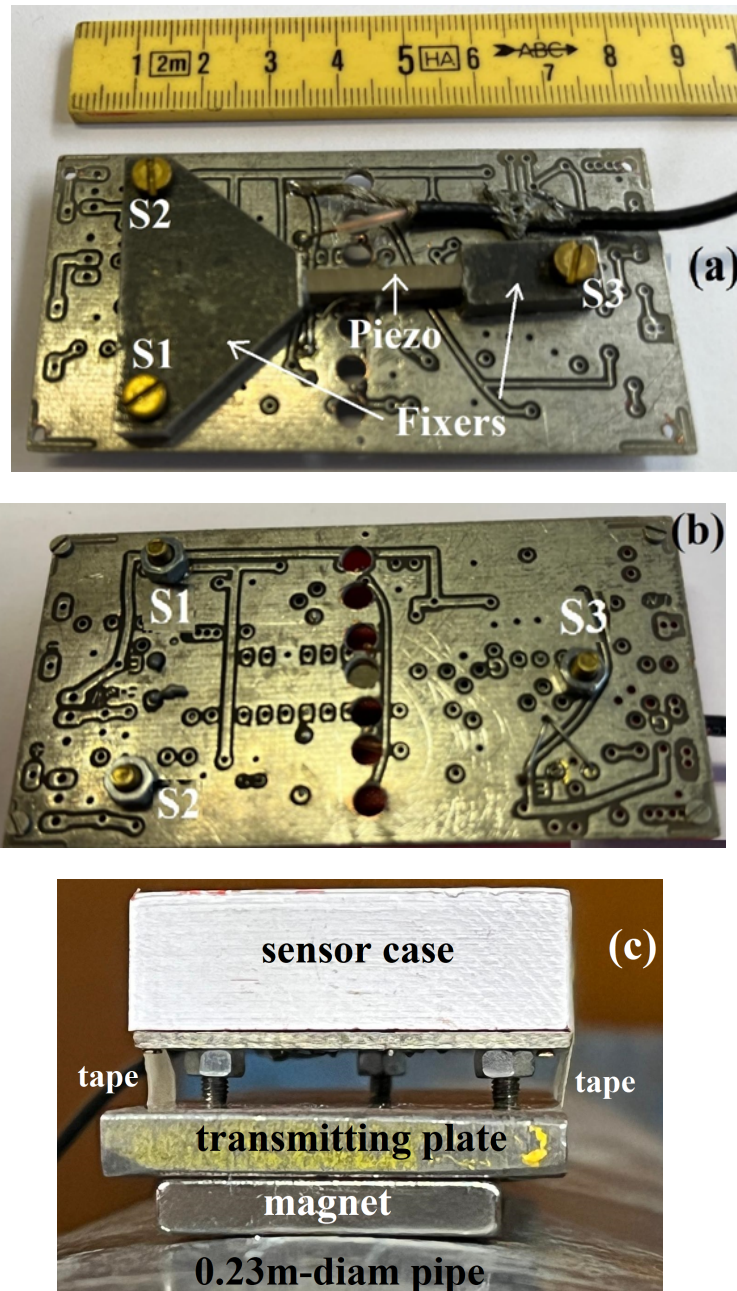


Fig. 1. Views of our sensor assembly. (a) Image of the top showing the piezo element, the fixers and the screws securing those to a PCB; (b) the back of the PCB showing the end of the screws; (c) cross section of the sensor assembly positioned on a 0.23m diameter pipe : below the sensor case three fixing screws contact the “transmission plate”. The strong magnet ($B=0.45\text{T}$) fixes the plate to the pipe and robust tape (indicated by side) secures the case to the transmitting plate .

The shape of the transmitting plate will always remain flat on the side where it must contact the three screws (and through the screws fixers and sensor), however, the rest of it can be shaped for the exigence of contacting objects of different solid geometries. For the experiments that we will present here, all devoted to test iron, or iron based metallic elements, using the magnets and the metal plate for securing the sensor assemblies to the elements resulted mechanically stable and reliable.

Let us discuss now the result of the first attempt that we made to detect the excitations induced in a steel pipe. In Fig. 2a we see a 5.5 m-long, 30 cm diameter, 1 cm thick pipe (white in the photo) laying on supports placed close to its ends. We fixed our sensor at one end of the pipe by the magnets while close to the other end we applied excitations just by letting a piece of metal weighting 10 g to fall on the pipe from a height of 2 cm. In these conditions the strength of the percussive excitation is 0.1 N and its potential energy of 1.96 mJ. The response of our sensor from the other end of the pipe is shown in Fig. 3 where we can see that it generates a burst of voltage pulses having a maximum amplitude modulus of 300 mV.

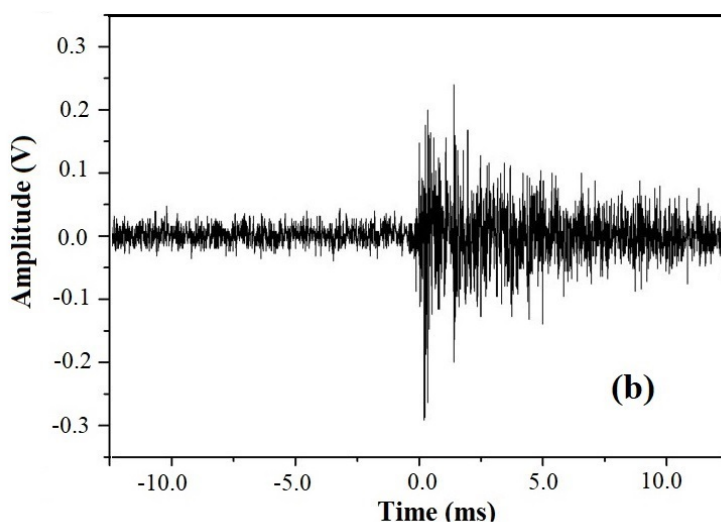
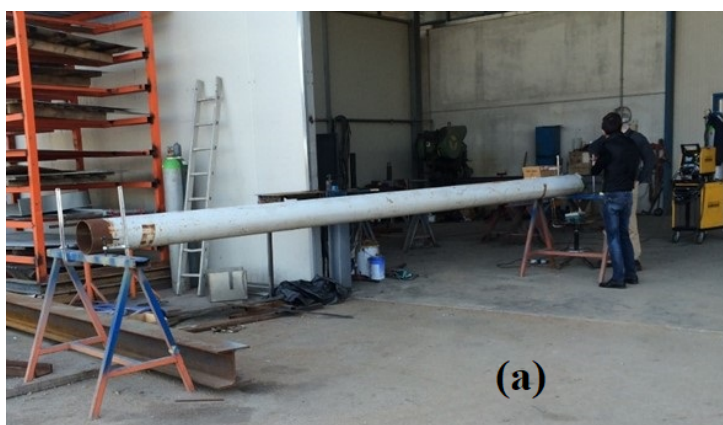


Fig. 2 . (a) Photo of the hollow pipe on which we first tested our sensor assembly. The pipe, white in color was held by two supports at its ends. The pipe length was 5.5 m, its diameter was 0.3 m and its thickness 0.01m ; (b) sensor response : negative values of the horizontal scale refer to the time before the sensor responded to the excitation which is zero on the scale.

A signal amplitude on the scale of hundreds of millivolt as the one we recorded, obtained for such a tiny excitation, is promising for detecting strong percussive effects generated kilometers away from the sensor. For this purpose, however, a prompt transmission from the piezo sensor (or from arrays of these) shall be important and a possibility to do it is to transmit information to remote sensors through ether. In the next section we will see how we have solved the problem of transmitting the information in remote.

3. Shaping Sensors Output Signal and Remote Sensing

Let us see now how is it possible to handle a signal such as the one shown in Fig. 2b to transform it into a rectangular pulse to be handled and eventually transmitted at a distance. When a vibration is detected by the piezoelectric the signal it generates is integrated by a charge amplifier (shaper) and then discriminated in amplitude and sent to a monostable multivibrator (one shot) to obtain a logic signal (trigger) having a fixed duration as shown in Fig. 3 where we see, in the upper trace the signal originated by the piezoelectric and in the lower trace the “treated” signal transformed into a trigger pulse.

In Fig. 4 a block scheme describes how the pulse of Fig. 3a (upper trace) can be transmitted to a remote receiver. The operation of the set up is as follows : in the normal state the transmitter is in the stand-by state and requires a very low current for its operation. When a vibration/excitation is detected the piezo generates a signal which is integrated by the charge amplifier (shaper), discriminated in amplitude and sent to a monostable vibrator (one shot) to obtain a logic signal (trigger) of predetermined duration, as shown in Fig. 3 (bottom). This signal is sent to one of the GPIO pins of a transmitter board which, receiving the signal, switches from the idle state (idle) to the transmission state (wake). The transmitted alarm signal, travelling on a high frequency carrier, is capable of traveling tens of kilometers in the ether and can consist of sending any string of characters preset during programming the board itself.

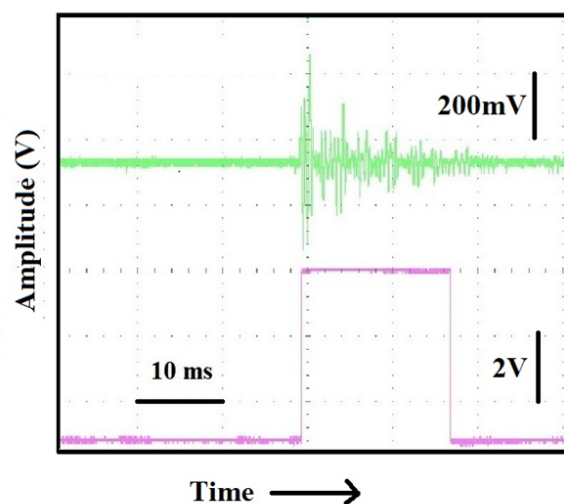


Fig. 3. Traces of the signal detected on a multichannel scope by our piezo sensor before (upper, green trace) and after the treatment to transform it in a 18 ms pulse ready to be conveyed to a transmitter (lower, violet trace). Vertical scales are 200 mV/div for the upper trace and 2V/div for the lower trace.

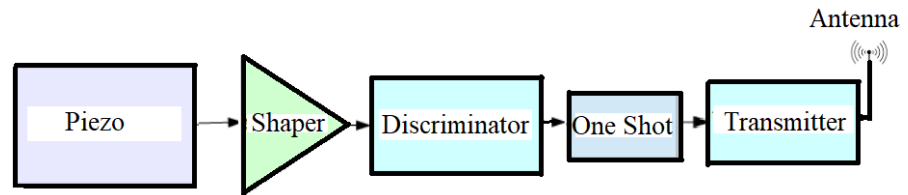
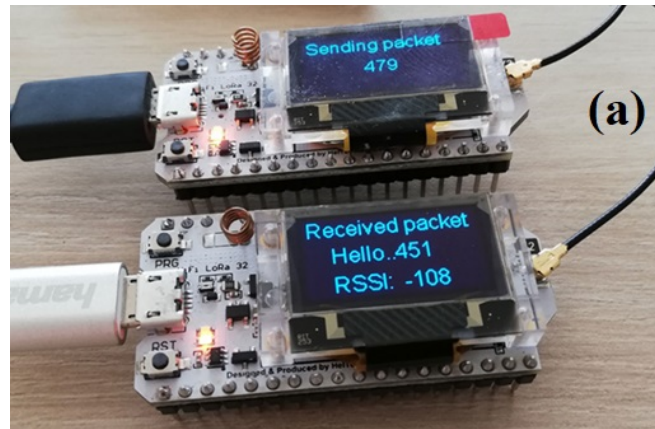


Fig. 4. Flow chart of the system we have set up in order to transmit in ether the signal generated by the piezoelectric sensor.

The block diagram of Fig. 4 was realized by a high-impedance charge amplifier LMC6041 Texas Instruments (the shaper), collecting the signal generated by the piezo and sending it to the fast discriminator LM311 Texas Instruments which, in the presence of a signal, above a preset threshold, causes a monostable (one-shot) multivibrator, to generate a logic pulse of a preset width from an RC network which represents the trigger signal. The one shot is realized with 2 NOR gates of IC 74HC02 along with capacitance and resistor determining the width of the pulse. The transmitter and receiver consist of a Heltec ESP32 LoRa V3 board, an advanced development module designed for IoT applications that integrate WiFi, Bluetooth and LoRa (Long Range) transmission connectivity in a very small size (50.2mm x 25.5 mm x 10.2 mm). Based on the ESP32-S3FN8 dual core Xtensa LX7 32-bit- 240 MHz microcontroller, it offers a powerful combination of performance and functionality.



```

sending packet "Tx_Rx Test 8, Rssi : -69" , length 24
TX done.....into RX mode

received packet "Tx_Rx Test 8, Rssi : -58" with Rssi -62 , length 24
wait to send next packet

sending packet "Tx_Rx Test 9, Rssi : -62" , length 24
TX done.....into RX mode

received packet "Tx_Rx Test 9, Rssi : -63" with Rssi -65 , length 24
wait to send next packet
  
```

Figure 5 : In the upper panel (a) we see the two transmitter and receiver boards in transceiver configuration; one is set in the “Sending Packet” mode, the other in the “Receiving Packet” mode; the lower panel (b) shows typical computer displays tracing the activity of the boards.

Semtech SX1276 LoRa chip-based integrated RF transmitter/receiver module support long range, low power (+22 dBm) communication [31,33]. Allowed radio transmission frequencies vary for different regions: 433 MHz (Asia), 868 MHz (Europe), 915 MHz (North America). Receiving sensitivity is -148dBm. Both boards, shown in Fig. 5, identical in size and features, can be programmed through USB interface in transmitter, receiver, or transceiver configuration. The boards can interface with microcontrollers through UART, SPI, or 12C communication ports. The receiver module can recognize which of the piezos placed on pipelines/bars has been stressed and thus which section of the elements has been affected by an event. This information is sent to a computer in real time. In receiver configuration the board gets the signals transmitted by the devices configured in transmission, decodes the data, and sends it to a microcontroller or computer for further processing and eventual on-screen display of both transmission parameters and data. In the lower panel of Fig. 5 in the first line Tx_Rx Test 8 indicate the test number for transmission (Tx) and receipt (Rx); the amplitude of the signals is recorded (-69 dBm) and also the time-length of the packet (24byte). Our “transmitting-receiving” protocol was checked to a distance of 300 m, but the same procedure was tested over hundreds of kilometers on space balloon atmospheric research; claims exist that the protocol has been tested at distances above of 1300 km [34]: this is not a scientific publication, and surely needs to be confirmed, but records in this competitive field are transmitted using the fastest media available for communication.

4. Characterization of Excitations on Pipes, Bars, and Ropes

Using the rectangle-shaped signals shown in sect. 3, the propagation of the acoustic excitations along pipes, bars and ropes are characterized and the velocity of sound in the three cases will now be extracted. Two sensors assemblies are positioned at different distances on the metallic structures and a light “pulse” of acoustic excitation is generated close to the ends of the structures as shown in Fig. 6.

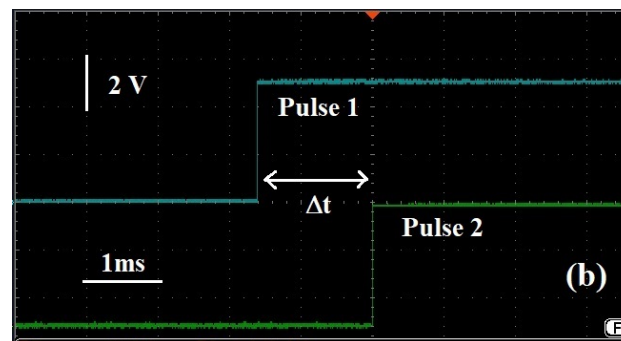
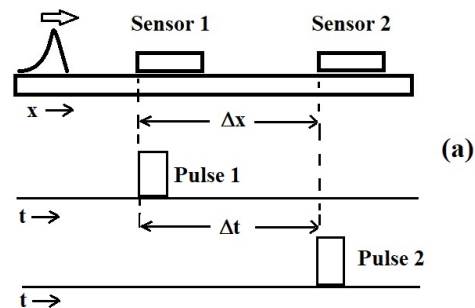


Figure 6 : (a) sketch of the protocol for measuring the time it takes to an acoustic excitation to cover the space between the two sensors; (b) bare oscilloscope display consequence of the process (a).

The output pulses of the two sensors feed two channels of a multi-trace oscilloscope (RSPRO IDS1104B, 100MHz) on which we read, and acquire, the two signals traces. The time taken to the excitations (idealized as wave packet with arrow on it in the figure) to travel between the two sensors is measured from time interval between the beginning of the pulses generated by the sensors as sketched in Fig. 6a. In practice, however, the time lengths of the pulses is much longer than the delay between them. Typical oscilloscope display from which one determines the time delays is shown in Fig. 6b where one can see just the rise of the two pulses and the time delay between them.

The measurement described in the previous paragraph were performed on a 6m-long iron pipe having a diameter of 3.3 cm and a thickness of 0.3 cm as shown in Fig. 7a. These results, like those for bars and ropes that will follow, were obtained positioning the sensors as shown in the inset of the figure, with the long direction of the transmission plate is parallel to the pipe. For the pipe the sensors were positioned at relative distances which were respectively 1.5 m, 3 m, 4.5 m and 5.5 m. The number of measurements, 10 at least, was increased when it was considered necessary to have more statistics. In spite of this, however, the statistical errors associated with the measurements are of the order of the symbol of the data in the plot. One can see that a linear relation between space and time delays exists and a least squares fit of the data returns a velocity $v_P = (3954 \pm 3.6\%) \text{ m/s}$.

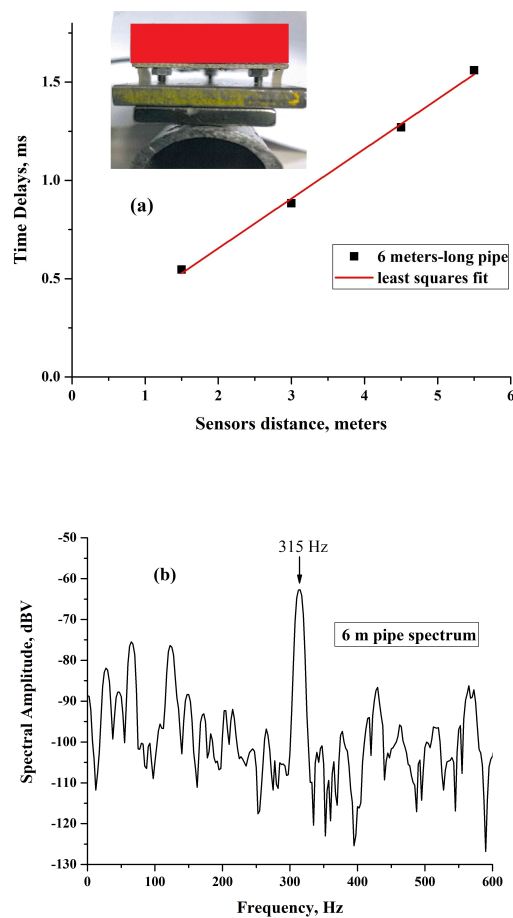


Figure 7: (a) dependence of the time delays between the pulses generated by two sensor assemblies on the 6m- pipe. The inset shows a photo of the cross section of sensor positioning with the long side of the transmitting plate parallel to the pipe; (b) low frequency spectrum showing the component corresponding to the fundamental frequency of the vibrating string model.

The fact that the velocity v_P corresponds to acoustic excitations travelling along the pipe was checked determining the spectrum of the pipe. As for the pulse delays measurement the spectrum was obtained applying a slight percussive excitation at the end of the pipe, but only one sensor was necessary in this case. In the portion of low-frequency spectrum shown in Fig. 7b one can see a component rising 45 dBV above the noise level at 315 Hz. This frequency, considering $L=6\text{m}$, can be identified as the fundamental frequency of the vibrating string pattern, namely $f=v_P/2L=329\text{ Hz}$: the two values (315 and 329 Hz) are consistent within the fitting error on v_P and the width of the spectral line. This frequency indeed can even be seen as the first harmonic of the Fourier spectrum of a pulse travelling back and forth along a finite length L .

Fig. 8a shows the results obtained placing the piezo sensors at distances of 1.5 m, 3 m, 4.5 m, and 5.5 m on a 6m-long, 0.8 cm diameter iron bar, of the type embedded in concrete in constructions. Even in this case a linear dependence of the time delays on the distance between the sensors is obtained. From the least square fit to the data and the consequent slope of the straight line a propagation velocity $v_B=(2470\pm1.7\%) \text{ m/s}$ is extracted.

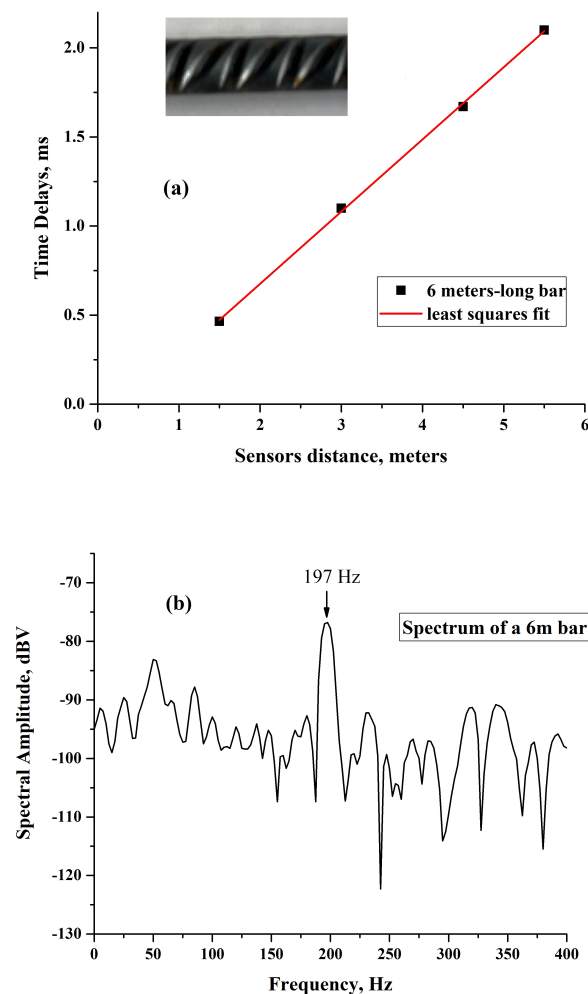


Figure 8: (a) time delays between sensors signal placed at different distances on an iron bar. The inset shows the bar surface (b) Low frequency spectrum (portion) of the excitations of the bar.

In Fig.8b we see that the low frequency spectrum of the bar exhibits a spectral line at 197 Hz , consistent, considering the errors in the velocity and the width of the spectral line, with the value expected for the fundamental mode of the free ends resonance of the bar obtained from the above extrapolated velocity and the length of the bar, namely $f = v_B / 2L = 206$ Hz.

The results obtained on a 4 m-long, 2 cm-diameter, seven wires galvanized steel rope purchased from MITARI Hijstechniek (Netherlands) are shown now in Fig. 9. The results were obtained positioning two sensors at distances of 1m, 2m, 3m , and 3.7m . When care is taken to apply excitations of the same power the results for the time delays are very reproducible. We can see that even here the results represent a linear dependence expected like in the previous cases, indicating a reliable relation between time and space.

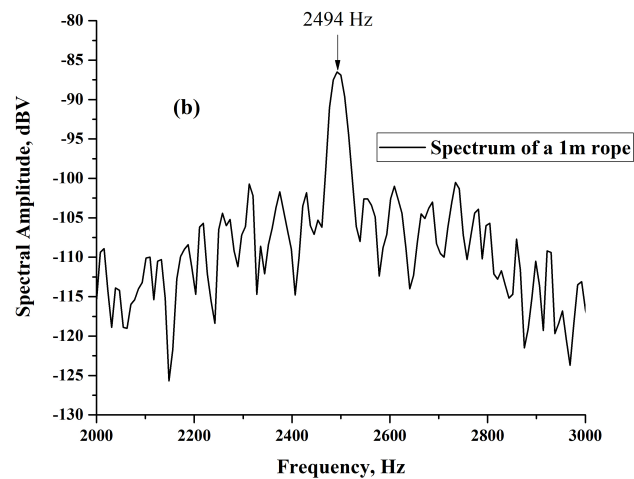
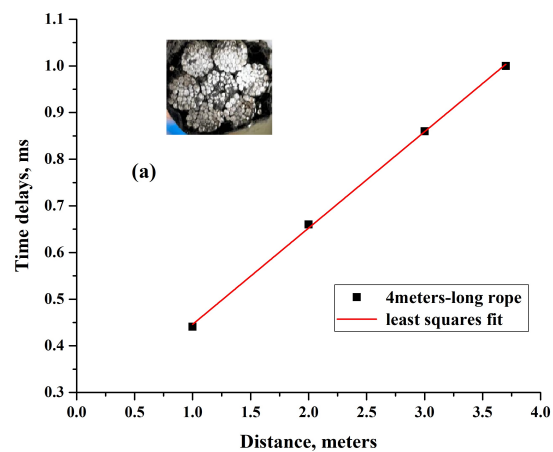


Figure 9 : (a) The time delays between the 4m-rope. The inset shows a section of the seven wires rope. (b) The spectrum of a 1m rope, consistent with the propagation velocity determined from the time delay measurements.

The line between the points is again a least squares fit to the data and from its slope we extract that the velocity of acoustic excitations in the rope is $v_R = (4830 \pm 1.6\%)$ m. Unfor-

fortunately, for the four meter rope it was not possible to observe the resonance in the spectrum as in the two previous cases. However, we did observe it on a one meter rope of the same batch and quality and the result is shown in Fig.9b : we can see in the figure a spectral line at 2494 Hz consistent within 3% with the frequency of the fundamental mode $f=v_R/2L$, expected from the above determination of v_R , and $L=1\text{m}$, here again the fundamental frequency of the excitation spectrum of the vibrating string model for a 1m rope.

The results of this section indicate that the detection protocol based on the generation of acoustic excitations, and their detection through piezo sensors, is reliable and consistent with the basic physical principles and the parameters that one can expect for the propagation of the excitations themselves along the three types of metallic structures. It is worth noting that the three structures investigated (pipe, bar, and rope) are substantially different in terms of geometric and structural point of view: this demonstrates the versatility of our piezo-sensors-based protocol for characterizing acoustic propagation. Specific examples will now be presented for the localization of excitations and defects along metallic structures and more examples of the signal traces on the oscilloscope will be shown.

5. Locating Excitations and Defects, Examples

For this section we will first consider two piezo sensors sticking on the 4m-galvanized steel rope used in the previous section. The outputs of the two piezo, discriminated to form squared impulses, feed, as before, two channels sharing the same time base of the multichannel scope. For the experiments that follows the signals generated by the two piezos where both treated to obtain pulses like those shown in Fig. 3. In the first experiment we used a 4 m steel rope and the transmitting plates, along with the piezos were positioned at 0.5 m from the ends of the rope. We note that the transmitting plates are 0.14 m long and we assume that the signals reach the sensors as soon as they excite the transmitting plate which means. that the in the experimental configuration shown in Fig. 10a in which we generate a light “parallel” percussive excitation on the rope as shown by the right-pointing arrow, the effective distance between the piezos is 2.86 m . PL and PR indicate the two piezos and their position: the letters L (Left) and R (Right) represent a convenient way for us to distinguish their position on the steel rope.

The result of the light percussion is shown in Fig. 10b. We see that the origin of the pulse of the piezo PR follows the one of PL after of 740 μs delay from which, given the distance between the two sensor assemblies. Indeed, an average over several measurements in this case returned time delay of 740 μs which is consistent with the plot of Fig. 8a. Repeating the experiment of Fig. 10b, but applying the “parallel” percussive excitation on the right end side of the rope we obtained results of the same order of magnitude. However, we must point out that it is difficult to estimate precise values of propagation speed in steel ropes by relying on percussive excitations and the related transmission of the signals along the ropes and this is evidenced in Fig. 10c. In this figure we show the time delay between the signals of the two piezos PL and PR measured when a light percussive excitation is applied on the rope in the center of the distance between the two sensors, as sketched by the down-pointing arrow in Fig. 10a. Now we would expect no delays between the start of the pulses, since the piezos are both at 1.43 m from the excitation point but, as we see in Fig. 10c, a 58 μs is measured.

The reason for the time delay in Fig.10c can be attributed to the fact that for the propagation paths of the acoustic excitation in the steel ropes one cannot expect the propagation velocities to be the exactly the same in the two directions when the percussive excitation is applied in direction orthogonal to the rope. As we shall see later in a steel bar the same type of experiment whose results are reported in From Fig. 10c exhibit delays of few microseconds.

The results of Fig. 10 indicate that an experimental set up such as the one of Fig. 10a gives the possibility to discriminate where a percussive excitation has been produced. These figures clearly indicate that the time delay between the origin of the piezo pulses scales with the relative distance of the piezos from the point where the excitations were generated and that the time delay is maximum when the excitation comes from a point external to the distance between the piezos.

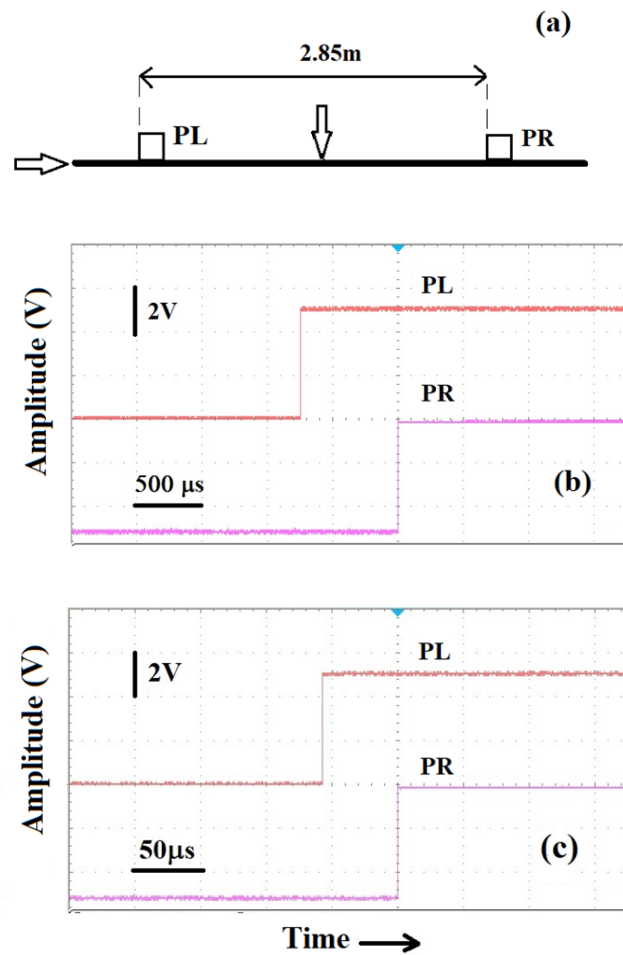


Fig. 10.(a) Sketch of the experiments performed for detecting time delays between piezos. (b) Delay of the origin of the pulses detected by the sensors assemblies secured at a relative distance of 2.86 m, visualized on a multichannel oscilloscope, when a light percussive excitation is generated at one end. (c) Time delay when percussion is applied at equal distance between the piezos assemblies. Vertical scales are same for the two traces in (b) and (c)

It is possible then that an array of piezos secured to a long bar, or rope, or pipe, can allow locating the position where an excitation is applied just from the minimum of the delays measured between all sensors. In other words, if signals are coming from a linear array of equally spaced sensors on a network of pipes, for example, the shortest time delay detected from two of these sensors will locate the origin of the excitation. Since the relative error on time measurements decreases for longer distances, is clear that this technique can increase in sensitivity and precision when the lengths of the metallic elements increases.

Let us see now how can be possible to locate defects along rope structures. In Fig. 11 we see, on the side panel, a photo of two steel ropes (one 2m long and another 4m long)

joint together by a strong magnet ($B=0.45\text{ T}$). In the same figure the response of the two sensors, positioned at 0.93 m from the discontinuity is shown. In this case an “orthogonal” percussive excitation was applied on the steel strand at half the distance (0.465 m) of the PR from the discontinuity. Now the delay in the response of the piezo on the other side of the rope is delayed of 2.1 ms , one order of magnitude with respect to what one can get from a continuous rope. Even in this case, inverting the positions of the sensors we obtained the same time delay.

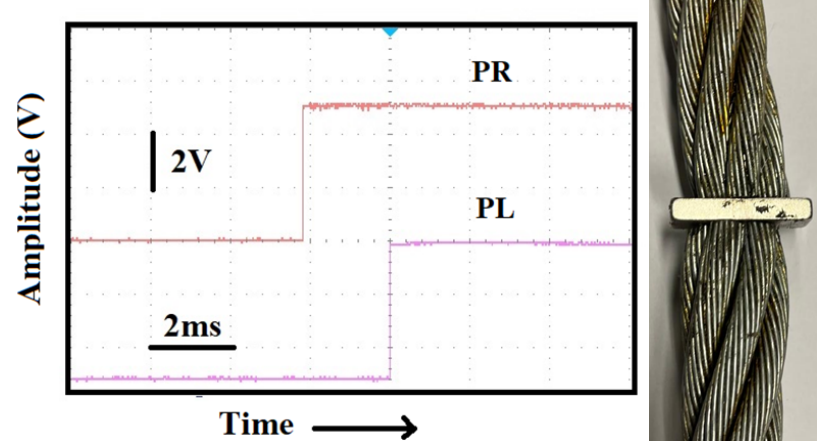


Fig. 11. Time delay (2.1 ms) measured when the two sensors are on the sides of a defect represented by a strong magnet holding the ropes together (see photo by side).

It is evident, from the substantially increased time delay between the origins of the pulses (2.1 ms), that the sensors are revealing the irregularity situated between the ropes. The same distance between the sensors (1.4 m) on a single, uninterrupted rope would generate a time delay roughly one order of magnitude shorter as we can tell from Fig. 9a. Thus, we speculate that, from measuring the time delays detected from an array of sensors placed at equal distances on bars, ropes or pipes, one could locate irregularities in these structures just from recording anomalous time delays between the two sensors closest to the defect.

The same kind of experiments described above were performed with cylindrical steel bar 0.007 m diameter, 1.41 m long steel bars. We anchored the two sensors on the steel bar at two centimeters from the ends of the bar itself and generated at one end “parallel” and “perpendicular” excitations. The result of a parallel percussive excitation generated at one end is shown in Fig. 12a and we see that the delay between the pulses is $430\text{ }\mu\text{s}$. Being the transmission plates long 14 cm and being these secured at 0.02 m from the ends of the bar the effective distance separating the sensors, from the point where the excitation reached the transmission plate on the first sensor to the point where the excitation is first detected on the second sensor is 1.23 m ; we note that this result is consistent with the data presented in the plot of Fig. 8a.

Generating a light, perpendicular, percussive excitation at one end of the bar we measured the same time delay between the signals generated by the two sensors. With the bar, however, a perpendicular excitation at half the distance between the sensors always gave a few microseconds delay confirming that the $58\text{ }\mu\text{s}$ delay in Fig.10c is very likely due to the specific structure of the ropes.

An artificial defect, with a rough cylindrical symmetry, 2.5 cm long and 1 mm deep, was then produced in the center of the bar used for the measurement of Fig. 12a. Now the time delays between the sensors assemblies secured, as before, at 2 cm from the ends of the bar are of $510\text{ }\mu\text{s}$ for “parallel” excitations at the right end of the bar while for “perpendicular” excitations, at the same end, delays slightly above 1 ms are measured, as shown in Fig. 12b. The delays measured clearly indicates the presence of an irregularity located

between the two sensors since without defect we got the same time delay for both perpendicular and parallel excitations while now for the parallel excitations we get a 15% increase of the delay and for the perpendicular excitations the delay increases more than a factor two.

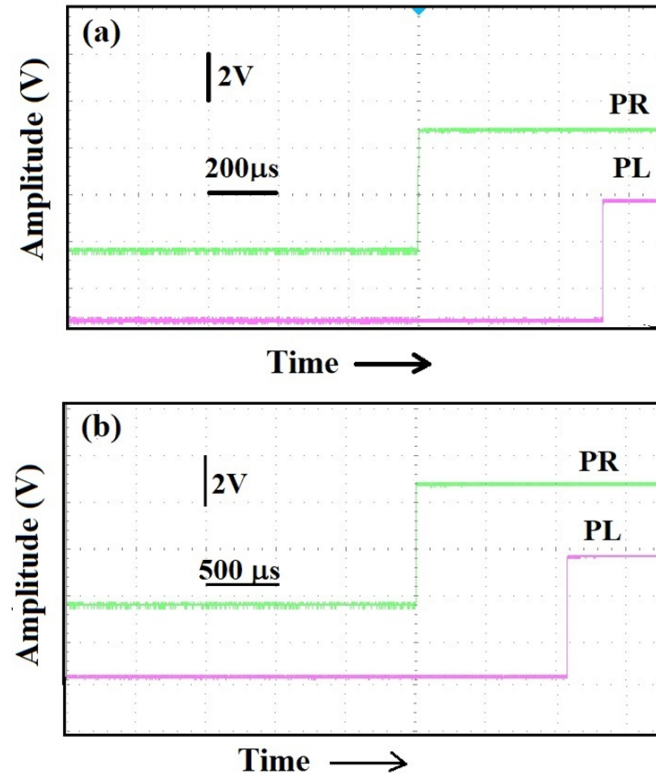


Fig. 12 : (a) time delay between sensors placed 2 cm away from a 1.41 m steel bar as a consequence of a parallel excitation. (b) time delay in the same positioning of the sensors in (a) when an artificial defect (see photo by side) is introduced.

5. Conclusions

Based on time-domain and frequency-domain measurements, it has been shown that piezo sensor assemblies can be effective in locating the position of excitations and defects of metallic objects. Attention has been concentrated on pipes, bars, and steel ropes. Although the ropes, due to their structure, represent a “tough” candidate for testing our detection mechanism, based on the propagation speed of excitations in solids, consistent results have been obtained even for ropes. Our proposed protocol could be adequate to satisfy cases in which non destructive analysis of the status of bars, ropes and pipes are necessary.

The sensitivity of our devices, their versatility and relatively low cost (we guess 500 € for each unit, including the transmitter) are such that building arrays of sensors to control rather extended networks like oil distribution pipelines can be conceived. As tool for transferring the excitations from the investigated elements to the piezo sensors we have employed a flat iron plate. This plate must always be flat on the side where it contacts the bottom of the three screws securing the sensor on the PCB, and transmitting excitations to it; however, the rest of the plate can be shaped/implemented in a way to improve the contact with specific metals geometries.

The analyses performed in sect.3, 4 and 5 show that transmission in the ether of the excitations signal (and the these start) from an array of sensors secured to bar, ropes or pipes can enable us to determine location of excitations and defects in remote assuming

naturally the fact that the speed of the transmission of em waves in the atmosphere is several orders of magnitude above what one has for sound waves in materials and therefore no further delays will be generated in the transmission and reception process. The time of the receiver board can be naturally synchronized to satellite signal in a way that the detection and the analyses can be recorded in real time.

We believe that our proposal is competitive and it is difficult to find something similar in literature : a system of 100 piezo sensors assemblies fixed every 10 km of pipeline, for example, could help monitoring 1000 km of oilduct with an economic load that has no match with any existing, or proposed, strategy/system. The cost of each of our sensor assembly , and signal treatment/ transmission of the piezo signal, is of the order of 500 euro. Unfortunately a “local” system capable of transmitting in real time information from large networks of elements such as pipelines conducts does not exist, and we hope it will be possible to implement a system based on the ideas herein presented.

6. Patents

Part of the work presented in the manuscript has been submitted to the *Ministero delle Imprese e del Made in Italy* for utility model patent (Application nr. 202024000005079).

Author Contributions: Conceptualization, M. C., E. R. and G.S.; methodology, MC.; validation, M. C., E. R. and G. S. ; resources, G. S.; data curation, M. C. and E. R.; writing—original draft preparation, M. C.; writing—review and editing, M. C. and E. R.; project administration, G. S.; funding acquisition, G. S. All authors have read and agreed to the published version of the manuscript.

Funding: This research was funded by AEGIS2k srl .

Institutional Review Board Statement: Does not apply

Informed Consent Statement: Does not apply

Data Availability Statement: Data presented are available, under request, from the corresponding author.

Acknowledgments: The design and the development of the sensor assembly herein presented was worked out in collaboration with prof. Massimiliano Lucci who suddenly left us on May 17, 2022. We hope that this paper can further honor his memory .

We thank Cadia D’Ottavi from Chemical Sciences and Technologies Department at the University “Tor Vergata” for the XRD characterization of the piezos material. Thanks are due to Antonio Lucia of the Nuova Impas company (Latina,Italy) for helping us to find a factory, the ATM Steel Technology in Latina (Italy), where we could test the sensors on the steel pipe as shown in Fig. 2. We thank the managers and the personnel of ATM for helping us to set up the tests.

Conflicts of Interest: The authors declare no conflicts of interest. The funders had no role in the design of the study; in the collection, analyses, or interpretation of data; in the writing of the manuscript; or in the decision to publish the results.

References

1. Tressler, J. F.; Alkoy, S.; Newnham R. E. Piezoelectric Sensors and Sensor Materials. *Journal of Electroceramics* **1998**, *2*, 257 .
2. Amprikidis, M. *Vibration Sensing Using Piezoelectric Devices and Signal Conditioning*; University of Manchester Ed. Manchester, U.K., 2004
3. Karbari, S. R.; Mohanram, S.; Sriniketh, S.; Uttara Kumari, M.; Shireesha, G.; “Signal conditioning circuits for low vibration signals using an array of piezoelectric sensors”, *Materials Today Proceedings* **2021**, *46*, 2212.
4. Denys Aguiar, O. Past, present and future of the Resonant-Mass gravitational wave detectors *Research in Astronomy and Astrophysics* **2011**, *11*, 1.
5. Dey, P. K. A risk-based model for inspection and maintenance of cross-country petroleum pipeline. *Journal of Quality in Maintenance Engineering* **2001**, *7*, 25, MCB University Press 1355-2511
6. Cunha, S. B. A review of quantitative risk assessment of onshore pipelines. *Journal of Loss Prevention in the Process Industries* **2016**, *44*, 282.

7. Aloqaily, A. Cross Country Pipeline Risk Assessments and Mitigation Strategies, Gulf Professional Publishing, an imprint of Elsevier, Cambridge, MA, USA, 2018. 486
8. Soomro, A A, Mokhtar, A A, Kurnia, J C, Lashari, N, Sarwar, U, Jameel, S M, Inayat, M & Oladosu, A review on Bayesian modeling approach to quantify failure risk assessment of oil and gas pipelines due to corrosion International Journal of Pressure Vessels and Piping **2022**, 200, 104841 . <https://doi.org/10.1016/j.iipvp.2022.104841> 487
9. Zhang P.; Qin G.; Wang Y. Risk, Assessment System for Oil and Gas Pipelines Laid in One Ditch Based on Quantitative Risk Analysis. *Energies* **2019**, 12, 981; doi:10.3390/en12060981. 488
10. Aljaroudi, A., Khan, F., Akinturk, A., Haddara, M., Thodi, P., Risk Assessment of Offshore Crude Oil Pipeline Failure. *Journal of Loss Prevention in the Process Industries* **2015**, 37,101 doi:10.1016/j.jlp.2015.07.004. 489
11. Simanjuntak, M.; Putro, U. Hydrocarbon Pipeline Third Party Damage Risk Assessment using Multi Criteria Decision Making. Proceedings of the International Conference of Business, Economy, Entrepreneurship and Management (IC-BEEM 2019), 579. ISBN: 978-989-758-471-8. 490
12. Kou, L.; Sysyn M.; Fischer S.; Liu J.; Nabochenko O. Optical rail surface crack detection method based on semantic segmentation replacement for magnetic particle inspection. *Sensors* **2022**, 21, 8214; doi: 10.3390/s22218214 491
13. Zhuang, L.; Wang, L.; Zhang, Z. Automated vision inspection of rail surface cracks: A double-layer data-driven framework. *Transportation Research Part C Emerging Technologies* **2018**, 92, 258 . 492
14. Gómez, M. J. ; E Corral , ; Castejon C.; García J. C. Prada Effective crack detection in railway axles using vibration signals and WPT energy. *Sensors*, **2018**, 18, 1603; doi:10.3390/s18051603 493
15. Liu, J.; Luo, H.; Hu, H.; Li, J. “Enhancing crack detection in railway tracks through AI-optimized ultrasonic guided wave modes”, *Biomimetic Intelligence and Robotics* **2024**, 4, 100175. 494
16. Amjad, U.; Yadav, S. K. ; Kundu, T. Detection and quantification of diameter reduction due to corrosion in reinforcing steel bars. *Structural Health Monitoring* **2015**, 14, 532. 495
17. Loveday, P. W.; Long, C. S. Laser vibrometer measurement of guided wave modes in rail track. *Ultrasonics* **2015**, 57, 209. 496
18. Zhou, P.; Zhou,G.; Zhu, Z; He, Z; Ding X.; C Tang C. A review of non-destructive damage detection methods for steel wire ropes. *Applied Sciences* **2019** , 9, 2771; doi:10.3390/app9132771. 497
19. Mazurek P.; Roskosz M.; Kwasniewski, J. Influence of the Size of Damage to the Steel Wire Rope on the Magnetic Signature *Sensors* **2022**, 22, 8162; <https://doi.org/10.3390/s22218162>. 498
20. Mazurek P.; Roskosz M.; Kwasniewski Novel diagnostic of steel wire rope with passive magnetic methods, *IEEE Magnetics Letters* **2021** PP(99):1-1 doi: 10.1109/LMAG.2021.3128828. 499
21. Hou, E. Z. Y.; Rostami, J.; Ng K. M.; Tse, P.W. Experimental Investigation on Choosing a Proper Sensor System for Guided Waves to Check the Integrity of Seven-Wire Steel Strands. *Sensors* **2020** ;20, 5025. doi: 10.3390/s20185025.PMID: 32899669 500
22. Čereška, A.; Kazimieras Zavadskas, E., Bucinskas, V.; Podvezko, V.; Sutiny's, E. Analysis of Steel Wire Rope Diagnostic Data Applying Multi-Criteria Methods, *Applied Sciences* **2018**, 8, 260; doi:10.3390/app8020260 501
23. Sutiny's, E.; Bucinskas, V.; Dziedzickis, A. The Research of Wire Rope Defect Using Contactless Dynamic Method. *Solid State Phenom.* **2016**, 251, 49. 502
24. Soh, C.K.; Bhalla, S. Calibration of piezo-impedance transducers for strength prediction and damage assessment of concrete. *Smart Mater. Struct.* **2005**, 14, 671. 503
25. Huo, L.; Cheng H.; Kong, Q.; Chen, X. Bond-Slip Monitoring of Concrete Structures Using Smart Sensors-A Review. *Sensors* **2019** 11;19(5):1231. doi: 10.3390/s19051231.PMID: 30862071 504
26. Damage Detection of Structures Based on Piezoelectric Sensors, Special Issue of Sensors (MDPI, C.E. Chalioris ed., 2020). Available online: https://www.mdpi.com/journal/sensors/special_issues/piezoelectri_sensor_detec 505
27. Karayannis, C. G. ; Chalioris, C. E.; Angeli, G. M.; Papadopoulos N. A. ; Favvata, M. J.; Providakis, C. P. Experimental damage evaluation of reinforced steel bars using piezoelectric sensors. *Constr. Build. Mater.* **2016**, 105, 227. 506
28. Providakis, C. P.; Karayannis, C. G.; Chariolis, C. E.; Favvata, M. J.; Angeli, G. M.; Papadopoulos, N. A. Usage of PZTs for damage evaluation of steel reinforcing bar. *Sch. J. Eng. Technol.* **2015**, 3, 80. 507
29. Mancini, M.;Turchetta, B.; Cirillo, M. Analysis of Properties and Macroscopic Defects of Metallic Bars, Pipes, and Strands through the Spectrum of Low-Frequency Excitations. *Materials* **2024**, 17, 2171; <https://doi.org/10.3390/ma17102171> 508
30. Ragini, R.; Ranjan, R.; Mishra, S. K.; Pandey, D. Room temperature structure of Pb(Zrx Ti1-x O3) around the morphotropic phase boundary region: A Rietveld study, *Journal of Applied Physics* **2002**, 92, 3266. 509
31. Escobar, J.J.L.; Gil-Castiñeira, F.; Díaz-Redondo, R. JMAC Protocol: A Cross-Layer Multi-Hop Protocol for LoRa. *Sensors* **2020**, 20, 6893. 510
32. Beltramelli, L.; Mahmood A.; Österberg, P.; Gidlund, M. LoRa beyond ALOHA: An Investigation of Alternative Random Access Protocols. *IEEE Transactions on Industrial Informatics* PP(99); doi: 10.48550/arXiv.2002.10732 511
33. Al mojamed M. On the Use of LoRaWAN for Mobile Internet of Things: The Impact of Mobility. *Appl. Syst. Innov.* **2022**, 5, 5; <https://doi.org/10.3390/asi5010005> 512
34. <https://www.hackster.io/news/another-record-breaking-transmission-for-lorawan-0cca5f6cd032#:~:text=For%20approximately%20three%20years%20now,had%20a%20LoRaWAN%20sensor%20attached> 513

Disclaimer/Publisher’s Note: The statements, opinions and data contained in all publications are solely those of the individual author(s) and contributor(s) and not of MDPI and/or the editor(s). MDPI and/or the editor(s) disclaim responsibility for any injury to people or property resulting from any ideas, methods, instructions or products referred to in the content.